Journal of Computer-Aided Molecular Design, 3 (1989) 299–309
ESCOM

J-CAMD 078

Atomistic lattice simulation of high T_c oxides

N.L. Allan* and W.C. Mackrodt**

ICI Chemicals and Polymers Ltd., PO Box 8, The Heath, Runcorn, Cheshire WA7 4QD, U.K.

Received 1 October 1989
Accepted 20 October 1989

Key words: Lattice simulation; Crystal structure; Defects; High T_c oxides

SUMMARY

A survey is outlined of some of the normal-state crystal properties of high T_c oxides that have been calculated recently by atomistic lattice simulations.

INTRODUCTION

Bednorz and Muller's [1] historic discovery of superconductivity in the system La-Ba-Cu-O at ~ 30 K has been followed by a period of intense activity in an attempt to understand the origins of this exotic behaviour. From a theoretical point of view much of this activity has been concerned with the coupling mechanism, often in the belief that it must necessarily differ from that of conventional superconductors. Rather less attention seems to have been paid to the fact that for much of the temperature-composition phase diagram of high T_c oxides they are quite normal ceramic materials and that it is likely that the normal-state properties are instrumental in determining their high T_c behaviour. Figure 1 shows this phase diagram for $La_{2-x}Sr_xCuO_4$ [2]. Three points are worth noting in this context. The first is that it is only for a narrow range of compositions that $La_{2-x}Sr_xCuO_4$ is superconducting and that the same is true for other high T_c oxides. The second is that the energy change at the superconducting transition for both high and low T_c materials is only of the order of 10^{-8} eV per atom so that the normal-state properties remain essentially unchanged in the superconducting state. The third is that the charge carriers in all the known high T_c materials are extrinsically controlled, either by impurities or oxidation/reduction, so that they are and can be treated as point defects in the accepted sense. In view of the likely continuity of normal-state lattice and defect properties in the superconducting regime, it has been argued previously [3–7] that valuable insight into the criteria for high T_c behaviour may be obtained

*Current address: Department of Theoretical Chemistry, University of Bristol, Bristol, U.K.
**To whom correspondence should be addressed.

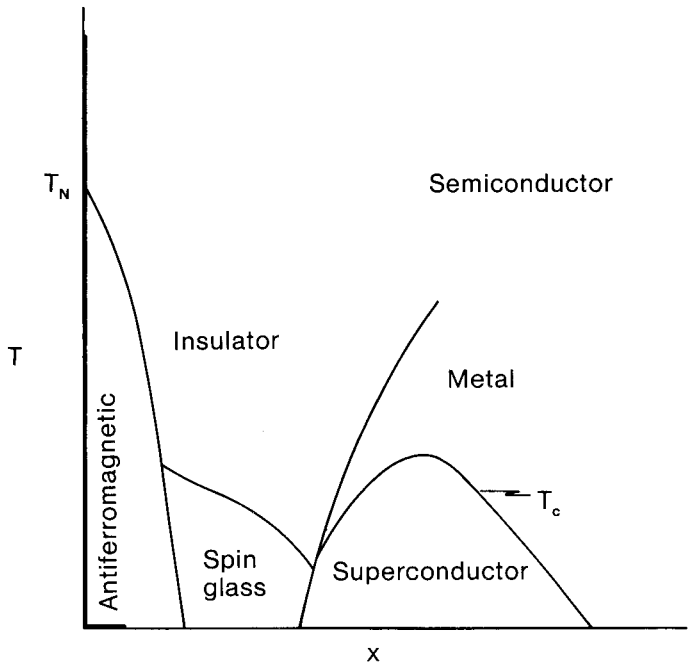

Fig. 1. Phase diagram for $La_{2-x}Sr_xCuO_4$.

from a study of these properties. This paper surveys some of the results of such studies based on recent atomistic lattice simulations by the present authors.

THEORETICAL METHODS

The theoretical methods used in these studies [3–7] are broadly similar to those used previously for a variety of ceramic oxides [8]. The calculations are formulated within the framework of an ionic model and are based on non-empirical two-body potentials derived from a modified electron–gas approximation [9]. Integral ionic charges associated with accepted chemical valence and electron counting were presumed throughout, i.e. 2+ for Cu, 3+ for La, 2− for O etc. This enables a simple definition of valence band holes as Cu^{3+} and O^- and defect electrons as Cu^+, and the useful concept of isovalent and aliovalent impurity substitution. An important feature of the potentials is the incorporation of the Dick–Overhauser shell model [10] for treating the electronic polarisation of the lattice. This plays an important role in determining both the structure and dynamics of the lattice and, as mentioned later, allows a description of free carriers in the large and small polaron limits.

Computer simulations are based on the methods of lattice statics for the energy and structure of perfect and defective lattices [11] and lattice dynamics [12] for the vibrational properties. The structure of perfect lattices is determined by the condition that it is in mechanical equilibrium i.e.,

$$\partial E/\partial X_i = 0 \tag{1}$$

where E is the internal energy, for all the variables, X_i, that define the structure. $\{X_i\}$ comprises the three lattice vectors $\{R_i\}$, the unit cell atomic positions $\{r_i\}$ and the shell displacements $\{s_i\}$. The

latter are non-zero for atoms/ions that are not at a centre of inversion symmetry in the lattice and, for highly polarisable ions such as O^{2-}, make an appreciable contribution to the stability of the lattice. For complex crystals it is sometimes convenient to minimise the internal energy initially for a subset of $\{X_i\}$, i.e. $\delta E/\delta r_i = 0$ for fixed $\{R_i\}$, which are often taken as the experimental lattice vectors; however, it is important to emphasise that at 0 K the zero strain structure is determined by Eq. (1) for all the variables X_i.

The most convenient approach to the simulation of defects in ionic lattices is that introduced by Lidiard and Norgett [13] and described in detail by Catlow and Mackrodt [11]. The essential concept is that the total energy of a defective system is minimised by a relaxation of the nuclear positions and shell displacements surrounding a defect. It is assumed that this relaxation is greatest in the immediate vicinity of the defect and that it falls off fairly rapidly at further distances away. This suggests a notional partition of the crystal into an inner region immediately surrounding the

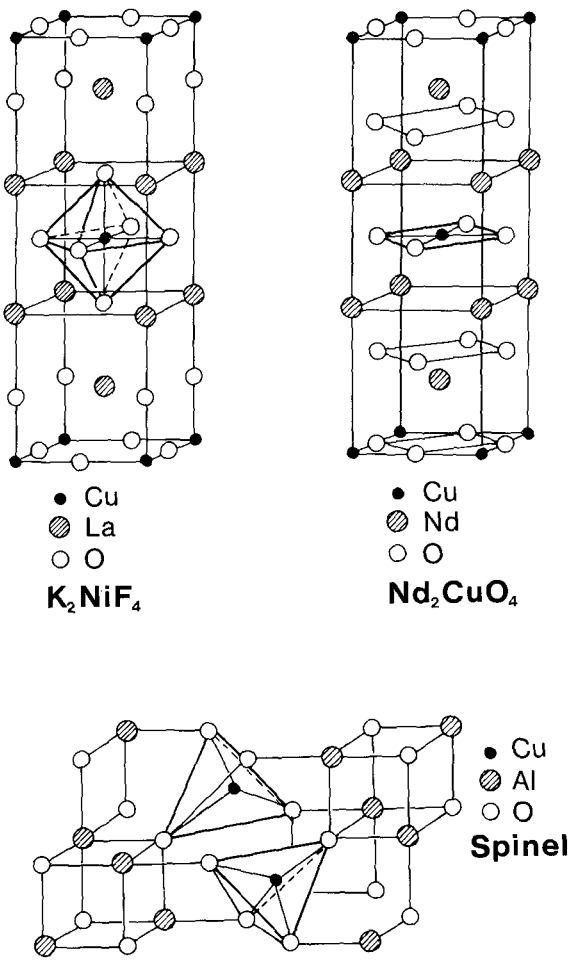

Fig. 2. Crystal structures of La_2CuO_4, Nd_2CuO_4 and Al_2CuO_4.

defect, which is appreciably distorted, and an outer region which is only slightly perturbed. In the former the relaxations are obtained by solving the appropriate elastic equations for the force explicitly, whereas those in the outer region are estimated from a suitable approxiation, the most useful being that suggested by Mott and Littleton [14]. Thus in the context of the general problem of point defects in solids, the two-region approach, as it is sometimes referred to, falls within the class of embedded-cluster models. The lattice dynamical methods are essentially those of Born and von Karman and extended by Cochran [12] to include the shell model. Phonon frequencies, and from these the densities of states, are obtained from the eigenvalues of the dynamical matrix which contains the second derivatives of the interatomic potential. Phonon frequencies are sensitive to the stability of the lattice and frequently when this is not at equilibrium imaginary frequencies are obtained.

CRYSTAL STRUCTURE

Early on, crystal structure was recognised as a key feature of high T_c oxides, with elements of the perovskite structure essential in providing the conducting CuO_2 planes and, it has been argued [3–7], the appropriate vibrational modes in the vicinity of 10 meV for electron-phonon coupling. Accurate computed structures, therefore, would seem to be an essential prerequisite for any theoretical approach to high T_c oxides. For La_2CuO_4, Nd_2CuO_4 and Al_2CuO_4, which is an example of a non-superconducting cuprate, we find the following structures in increasing energy:

La_2CuO_4: orthorhombic K_2NiF_4 < tetragonal K_2NiF_4 < Nd_2CuO_4 < lenips * < spinel

Nd_2CuO_4: Nd_2CuO_4 < tetragonal K_2NiF_4 < lenips < spinel

Al_2CuO_4: spinel < lenips < Nd_2CuO_4 < tetragonal K_2NiF_4

TABLE 1

CALCULATED AND EXPERIMENTAL LATTICE PARAMETERS OF M_2CuO_4 (M = La, Nd, Al) AND M_2CuO_3 (M = Ca, Sr)

Oxide	Structural type		Lattice parameters (A)		
			a	b	c
La_2CuO_4	Orthorhombic K_2NiF_4	Ref. 26	5.427	5.352	12.994
			(5.406)	(5.370)	(13.150)
La_2CuO_4	Tetragonal K_2NiF_4	Ref. 27	3.783	–	13.050
			(3.778)		(13.093)
Nd_2CuO_4	Nd_2CuO_4	Ref. 28	3.898	–	11.985
			(3.945)		(12.171)
Al_2CuO_4	Spinel	Ref. 29	8.025	–	–
			(8.064)		
Ca_2CuO_3	Sr_2CuO_3	Ref. 30	3.688	3.256	12.553
			(3.779)	(3.259)	(12.239)
Sr_2CuO_3	Sr_2CuO_3	Ref. 31	3.892	3.474	13.067
			(3.91)	(3.48)	(12.69)
$Bi_2Sr_2CaCu_2O_8$	Tetragonal	Ref. 32	3.773	–	31.045
			(3.83)		(30.89)

*Inverse spinel.

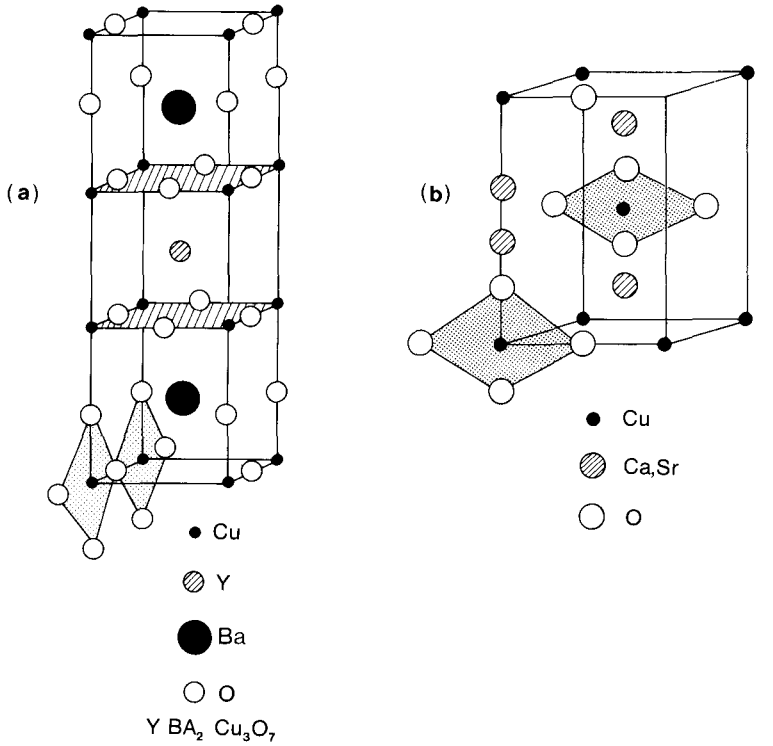

Fig. 3. Crystal structures of $YBa_2Cu_3O_7$ and Ca_2CuO_3.

Thus in each case we predict the correct crystal structures, shown in Fig. 2, with calculated lattice parameters given in Table 1. Reference to Fig. 2 shows that both La_2CuO_4 and Nd_2CuO_4 contain the putative (super)conducting CuO_2 planes so that while crystal structure is evidently important, an explanation of the difference in the high T_c behaviour of these materials needs to be sought beyond the lattice structure. Recently [5] we raised the question as to whether high T_c behaviour could be exhibited by systems containing not CuO_2 planes, as in La_2CuO_4 and Nd_2CuO_4, but CuO_2 chains of the type that are present in $YBa_2Cu_3O_{6.5+x}$ and shown shaded in Fig. 3a. Two such systems are Ca_2CuO_3 and Sr_2CuO_3, the structure of which is shown in Fig. 3b, and calculated lattice parameters given in Table 1. The significance of superconducting CuO_2 chains, if they exist, is that they would eliminate at least one of the suggested antiferromagnetic coupling mechanisms that have been proposed for high T_c cuprates [15]. As yet it is not known whether Ca_2CuO_3 and Sr_2CuO_3 lead to high T_c superconductors. The final materials we consider in this section on crystal structure are those that are contained within the system Bi-Sr-Ca-Cu-O with T_c's in excess of 100 K. They are shown schematically in Fig. 4 and the calculated lattice parameters listed in Table 1. These materials are also characterised by CuO_2 planes, with Cu both 4- and 5-fold coordinated, though it is not known at present whether this leads to differences in the superconducting properties of the individual planes. However, the main point to which we wish to draw attention here is that, as Table 1 shows, for the entire range of materials considered, the theoretical methods outlined in the previous section predict accurate crystal structures with calculated lattice parameters that are within 2% of the measured values.

PHONONS

The most recent reports of high T_c superconductivity in $Ba_{1-x}K_xBiO_3$ [16] (3-dimensional superconductivity), Ce-doped Nd_2CuO_4 [17, 18] (electron superconductivity) and in La_2NiO_4 [19] ($S \neq 1/2$) have cast doubts on some of the most sophisticated theories of coupling so that, as Bardeen [20], with some insight (!), has pointed out, phonons might (still) play a role in high T_c behaviour. In the case of $La_{2-x}Sr_xCuO_4$ there is both theoretical and experimental evidence for hole-lattice coupling associated with a strong peak in the phonon density of states at ~ 10 meV [21, 22], which is also present in the parent oxide [23]. In view of this we have suggested that a strong peak in the vicinity of 10 meV might be a possible prerequisite for phonon-mediated high T_c behaviour [3–7]. Figure 5 shows the calculated phonon densities of states for $La_{2-x}Sr_xCuO_4$, Nd_2CuO_4, $Bi_2Sr_2CaCu_2O_8$ and $SrTiO_3$ compared with that of La_2CuO_4. The three high T_c materials appear to possess the putative phonon states in common with $SrTiO_3$, which, as mentioned above, suggests that elements of the perovskite structure are important for their dynamic properties in addition to the provision of the conducting planes.

CHARGE CARRIERS

A feature of high T_c materials that appears not to have been emphasised sufficiently is that in every case the charge carriers, whether electrons or holes, are *extrinsic* as a result of doping, as in La_2CuO_4 and Nd_2CuO_4, or oxidation/reduction, as in $YBa_2Cu_3O_{6.5+x}$. High T_c superconductivity, therefore, is essentially a phenomenon involving defect electrons and holes. Atomistic simulation methods allow estimates to be made of the energies, which determine the type and stability of the various charge carriers, and the dielectric properties, which play an important role in their coupling, whatever the mechanism. As mentioned earlier, the shell model allows a quantitative distinction to be made between descriptions of free carriers, either holes or defect electrons, in the large and small polaron limits and from these quantitative estimates of the carrier-lattice coupling

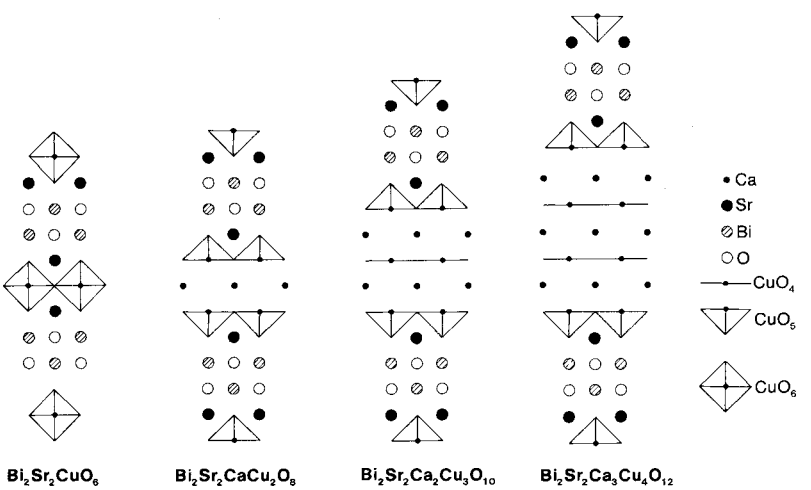

Fig. 4. Crystal structures of materials within the system Bi-Sr-Ca-Cu-O.

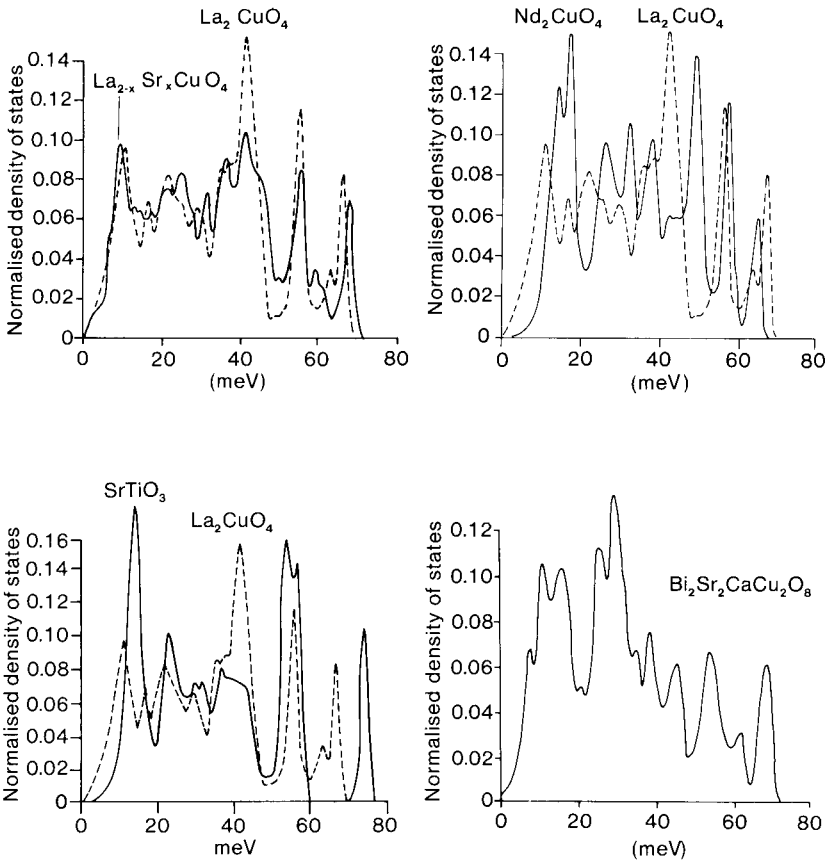

Fig. 5. Calculated phonon densities of states of $La_{2-x}Sr_xCuO_4$, Nd_2CuO_4, $Bi_2Sr_2CaCu_2O_8$ and $SrTiO_3$ compared with that of La_2CuO_4.

energies. Technically, this is done in the following way. The lattice contribution to the large polaron energy comprises solely an (electronic) polarisation term, which is obtained by fixing the atomic positions, $\{r_i\}$, and allowing the shell displacements, $\{s_i\}$, to equilibrate; whereas the small polaron energy includes both the shell displacements and nuclear relaxation contributions. We have previously pointed out that while the polaron concept is essentially dynamic in nature, since it involves the coupling of the carrier to the oscillating electric field of a vibrating polar lattice, the use of static lattice calculations can be justified on the grounds that a static description, which can be thought of as the zero-frequency limit of the dynamic case, contains the essential physics of the problem [24,25]. Table 2 lists the calculated electronic defect structures and energies for La_2CuO_4, Nd_2CuO_4, Al_2CuO_4, Ca_2CuO_3 and Sr_2CuO_3. We predict Cu 3d holes in La_2CuO_4 and Al_2CuO_4 and O 2p holes in the remainder. However, in every case the difference in energy between the two types of hole is small, particularly in relation to the approximations made in estimating hole formation energies. This, we have argued [3], might reasonably be interpreted as suggesting valence band holes of mixed character, reflecting the strong pdσ nearest-neighbour interaction between Cu $3d_{x-y}$ and O $2p_{x,y}$ orbitals. We also predict strong carrier-lattice coupling, with energies in the

TABLE 2

THE CALCULATED ELECTRONIC DEFECT STRUCTURE AND ENERGIES OF La_2CuO_4, Nd_2CuO_4, Al_2CuO_4, Ca_2CuO_3 AND Sr_2CuO_3

Defect properties/energies (eV) Structural type	La_2CuO_4 Orthorhombic	Nd_2CuO_4 Nd_2CuO_4	Al_2CuO_4 Spinel	Ca_2CuO_3 Sr_2CuO_3	Sr_2CuO_3 Sr_2CuO_3
Valence band holes/formation energy[a]	$^{l}h_{Cu}$ 1.8 $^{s}h_{Cu}$ 2.0 $^{l}h_{O}$ 3.0	$^{l}h_{O}$ 3.1 $^{s}h_{O}$ 4.2 $^{s}h_{Cu}$ 4.3	$^{l}h_{Cu}$ 5.8 $^{s}h_{Cu}$ 6.1 $^{l}h_{O}$ 6.4	$^{l}h_{O}$ 3.3 $^{s}h_{O}$ 5.1 $^{l}h_{Cu}$ 4.2	$^{l}h_{O}$ 2.4 $^{s}h_{O}$ 4.2 $^{l}h_{Cu}$ 3.9
Difference in energy between lowest energy holes	1.2	1.2	0.6	0.9	1.5
Defect electron/formation energy[b]	$^{s}e_{Cu}$ 2.4	$^{s}e_{Cu}$ −0.9	$^{l}e_{Cu}$ −0.6	$^{s}e_{Cu}$ −0.7	$^{s}e_{Cu}$ −0.8
band gap[c]	4.2 (~3)	2.2 (1.6)	5.2	2.6	1.6
Electron/hole – lattice coupling energies:					
hole	1.1–1.7	1.0–1.7	1.1	1.2–1.5	1.2–1.8
electron	1.2	1.2	0.6	1.4	1.5

[a]For example $^{l}h_{Cu}$ denotes a large polaron hole on Cu.

[b]Defect equals empty conduction band.

[c]Experimental values for La_2CuO_4 [33] and Nd_2CuO_4 [34] in parentheses.

range 1.0–1.8 eV, leading to relatively small differences in energy between large and small polaron holes and defect electrons. Thus, our calculations are supportive of Bardeen's view [20] that carrier-phonon coupling makes some contribution to high T_c superconductivity.

OXIDATION-REDUCTION

The oxidation state and the nature and stability of the associated defects are major factors that control the behaviour of oxide superconductors. The most significant features are the stability of

TABLE 3

CALCULATED OXIDATION-REDUCTION ENERGIES (eV) OF La_2CuO_4, Nd_2CuO_4, Ca_2CuO_3 AND Sr_2CuO_3

Energy	La_2CuO_4	Nd_2CuO_4	Ca_2CuO_3	Sr_2CuO_3
(a) Low temperature limit				
E_1	−1.7	0.1	−0.5	−1.3
E_2	10.4	−0.7	2.7	1.6
E_3	4.4	0.5	1.4	0.5
(b) At 1000 K				
E_1	−0.5	1.3	0.7	−0.1
E_2	8.6	−2.5	1.5	0.4
E_3	3.2	−0.7	0.2	−0.7

TABLE 4

CALCULATED SOLUTION ENERGIES (eV) OF THE ALKALINE-EARTH OXIDES IN La_2CuO_4

Oxide	E_{La}	E_{Cu}
MgO	2.4	0.8
CaO	0.3	4.0
SrO	−0.3	7.3
BaO	−0.1	11.0

holes with respect to oxygen vacancies and (defect) electrons with respect to cation vacancies via the following reactions,

$$V_O^{\cdot\cdot} + 1/2O_2(g) \rightleftharpoons O_O^x + 2h^{\cdot}$$
$$V_M'''(V_M'') + 3/2(1)\, O_O^x \rightleftharpoons 3/4(1/2)\, O_2(g) + 3(2)\, e'$$

and $$V_{Cu}'' + O_O^x \rightleftharpoons 1/2\, O_2(g) + 2\, e'$$

with energies E_1, E_2 and E_3, respectively. These are listed in Table 3 in the low-temperature limit (a) and at 1000 K (b) for La_2CuO_4, Nd_2CuO_4, Ca_2CuO_3 and Sr_2CuO_3. Allowing for the approximations involved in calculating the various contributions to E_1, E_2 and E_3, which lead to uncertainties of several tenths of an eV [3–7], we find holes to be stable in La_2CuO_4, Ca_2CuO_3 and Sr_2CuO_3 and electrons in Nd_2CuO_4. Thus on stability grounds alone, La_2CuO_4 would be expected to lead to hole superconductors and Nd_2CuO_4 to electron superconductors in agreement with the known behaviour of these materials [1, 2, 16, 17].

CATION IMPURITIES

As mentioned earlier, the charge carriers in all the known high T_c oxides are extrinsic as a result of doping or oxidation/reduction. The cation doping characteristics, therefore, are of prime importance and, in particular, the mode of solution, for it is this that determines whether or not extrinsic carriers are created. To illustrate this point we consider the doping of La_2CuO_4 by MgO, CaO, SrO and BaO and Nd_2CuO_4 by ZrO_2, CeO_2 and ThO_2. For Cu substitution the relevant defect reactions are

TABLE 5

CALCULATED SOLUTION ENERGIES (eV) OF ZrO_2, CeO_2 AND ThO_2 IN Nd_2CuO_4

Oxide	E_{Cu}	E_{Nd}
ZrO_2	10.1	1.5
CeO_2	10.8	1.1
ThO_2	10.9	1.4

$$XO + Cu^{x}_{Cu} \rightleftharpoons X^{x}_{Cu} + Cu^{x}_{Cu} + O^{x}_{O}$$

and $$XO_2 + Cu^{x}_{Cu} \rightleftharpoons X^{\cdot\cdot}_{Cu} + 2e' + 1/2\,O_2(g) + Cu^{x}_{Cu} + O^{x}_{O}$$

and for La/Nd substitution

$$XO + La^{x}_{La} + 1/4\,O_2(g) \rightleftharpoons X'_{La} + h^{\cdot} + La^{x}_{La} + 3/2\,O^{x}_{O}$$

and $$XO_2 + Nd^{x}_{Nd} \rightleftharpoons X^{\cdot}_{Nd} + e' + 1/4\,O_2(g) + Nd^{x}_{Nd} + 3/2\,O^{x}_{O}$$

Tables 4 and 5 contain the calculated solution energies. We see immediately that Ca, Sr and Ba are predicted to substitute the La-sublattice in La_2CuO_4 with the creation of holes as compensating defects, which couple to give superconducting Cooper pairs. Mg, on the other hand, is predicted to substitute for Cu isovalently and hence cannot lead to a superconducting material. Likewise, Zr, Ce and Th are predicted to substitute for Nd in Nd_2CuO_4, with the creation of (defect) electrons, thereby leaving intact the (super)conducting CuO_2 planes. Calculations of this type [3] have also predicted that the doping of La_2CuO_4 by Na_2O, but not Li_2O, would lead to the creation of holes and hence to materials with potential high T_c properties and that Al as an impurity in La_2CuO_4-based materials would have a deleterious effect on the superconductivity for it would substitute for Cu rather than La, thereby disrupting the conducting planes, and also suppress the hole concentration [3].

CONCLUSION

The purpose of this brief survey has been to show that atomistic lattice simulations of the type that have been used previously for examining conventional ceramic materials are able to calculate important normal-state properties of high T_c oxides that are relevant to superconducting behaviour.

REFERENCES

1 Bednorz, J.G. and Muller, K.A., Z. Phys. B. (Condensed Matter), 64 (1986) 189.
2 Birgenau, R.J., Kaster, M.A. and Aharony, A., Z. Phys. B (Condensed Matter), 71 (1988) 57.
3 Allan, N.L. and Mackrodt, W.C., Phil. Mag., A58 (1988) 555.
4 Allan, N.L., Lawton, J.M. and Mackrodt, W.C., Phil. Mag., B59 (1989) 191.
5 Allan, N.L., Lawton, J.M. and Mackrodt, W.C., J. Phys. (Condensed Matter), 1 (1989) 2657.
6 Mackrodt, W.C., Mol. Simul., 3 (1989) 1.
7 Allan, N.L. and Mackrodt, W.C., J. Chem. Soc., Faraday Trans. 2, 85 (1989) 383.
8 Mackrodt, W.C., Solid State Ionics, 12 (1984) 175.
9 Mackrodt, W.C. and Stewart, R.F., J. Phys., C12 (1979) 431.
10 Dick, B.G. and Overhauser, A.W., Phys. Rev., 112 (1958) 90.
11 Catlow, C.R.A. and Mackrodt, W.C., In Catlow, C.R.A. and Mackrodt, W.C. (Eds.) Computer Simulation of Solids, Springer-Verlag, Berlin, 1982.
12 Cochran, W., Crit. Rev. Solid State Sci., 2 (1977) 1.
13 Lidiard, A.B. and Norgett, M.J., In Herman, F.H., Dalton, N.W. and Koehler, T.R. (Eds.) Computational Solid State Physics, Plenum Press, New York, 1972.
14 Mott, N.F. and Littleton, M.J., Trans. Faraday Soc., 34 (1938) 485.
15 Hirsch, J.E., Phys. Rev. Lett., 59, (1987) 228.

16 Cava, R.J., Batlogg, B., Krajewski, J.J., Farrow, R., Rupp, Jr., L.W., White, A.E., Short, K., Peck, W.F. and Kometani, T., Nature, 332 (1988) 814.
17 Tokura, Y., Takagi, H. and Uchida, S., Nature, 337 (1989) 3457.
18 Takagi, H., Uchida, S. and Tokura, Y., Phys. Rev. Lett., 62 (1989) 1197.
19 Kakol, Z., Spalek, J. and Honig, J.M., J. Solid State Chem., 79 (1989) 288.
20 Bardeen, J., Mat. Res. Soc. Symp. Proc., 99 (1988) 27.
21 Weber, W., Phys. Rev. Lett., 58 (1987) 1371.
22 Ramirez, A.P., Batlogg, B., Aeppli, G., Cava, R.J., Rietman, E., Goldman, A. and Shirane, G., Phys. Rev., B35 (1987) 8833.
23 Balakrishnan, G., Berhoeft, N.R., Bowden, Z.A., Paul, D.McK. and Taylor, A.D., Nature, 327 (1987) 45.
24 Anderson, P.W., Phys. Rev. Lett., 34 (1975) 953.
25 Chakravorty, B.K., J. Phys. (Paris), 42 (1981) 1351.
26 Grande, B. and Müller-Buschbaum, Hk., Z. Anorg. Allg. Chem., 417 (1975) 68.
27 Longo, J.M. and Raccah, P.M., J. Solid State Chem., 6 (1979) 526.
28 Müller-Buschbaum, Hk. and Wollschlager, W., Z. Anorg. Allg. Chem., 414 (1975) 76.
29 Wyckoff, R.W.G., Crystal Structures, Vol. 3, 2nd ed., Interscience, New York, 1963, p. 78.
30 Teske, Chr.L. and Müller-Buschbaum, Hk., Z. Anorg. Allg. Chem., 371 (1969) 325.
31 Teske, Chr.L. and Müller-Buschbaum, Hk., Z. Anorg. Allg. Chem., 379 (1970) 234.
32 Bordet, P., Chaillout, J.J., Chenavas, J., Hewat, A.W., Hewat, E.A., Hodeau, J.L., Marezio, M., Tolence, J.L. and Tranqui, D., Physica C153–155 (1988) 623.
33 Reihl, B., Riesterer, T., Bednorz, J.G. and Muller, K.A., Phys. Rev., B35 (1987) 8804.
34 George, A.M., Gopalkrishnan, I.K. and Karkhanavala, M.D., Mater. Res. Bull., 9 (1974) 721.